

# Reconstruct! Don't Encode: Self-Supervised Representation Reconstruction Loss for High-Intelligibility and Low-Latency Streaming Neural Audio Codec

Junhyeok Lee <sup>1,\*\*</sup>, Xiluo He <sup>1</sup>, Jihwan Lee <sup>2</sup>, Helin Wang <sup>1</sup>, Shrikanth Narayanan <sup>2</sup>,  
Thomas Thebaud <sup>1</sup>, Laureano Moro-Velazquez <sup>1</sup>, Jesús Villalba <sup>1</sup>, Najim Dehak <sup>1,\*\*</sup>

<sup>1</sup> Center for Language and Speech Processing, Johns Hopkins University, USA

<sup>2</sup> Signal Analysis and Interpretation Laboratory, University of Southern California, USA

jlee843@jhu.edu, ndehak3@jhu.edu

## Abstract

Neural audio codecs optimized for mel-spectrogram reconstruction often fail to preserve intelligibility. While semantic encoder distillation improves encoded representations, it does not guarantee content preservation in reconstructed speech. In this work, we demonstrate that self-supervised representation reconstruction (SSRR) loss fundamentally improves codec training and performance. First, SSRR significantly accelerates convergence, enabling competitive results using only a single GPU. Second, it enhances intelligibility by reconstructing distilled self-supervised representations from codec outputs. Third, SSRR enables high intelligibility without additional lookahead in streaming Transformer-based codecs, allowing a zero-lookahead architecture for real-time deployment. As a result, our JHCodec achieves state-of-the-art performance while maintaining minimal latency and reduced training cost. We open-source the full implementation, training pipeline, and demo on GitHub<sup>1</sup>.

**Index Terms:** neural audio codec, streaming model, self-supervised representation

## 1. Introduction

The rapid evolution of audio and speech large language models [1–5] has redefined speech synthesis as a scalable autoregressive language modeling problem. This paradigm is fundamentally built upon speech representations, especially neural audio codecs, which serve as tokenizers to compress high-dimensional continuous waveforms into sequences of discrete tokens [6–8]. These codecs typically employ vector-quantized variational autoencoders (VQ-VAE) [9], with various design choices ranging from single large codebooks [10–13] to multi-stage residual vector quantization (RVQ) [4, 6–8], alongside alternative approaches like finite scalar quantization (FSQ) [14] or binary representations [15, 16]. They are mainly trained with reconstruction objectives, such as multi-scale mel-spectrogram losses, often combined with waveform losses or generative adversarial networks (GANs) [17] following prior neural vocoders [18–20], to improve perceptual quality.

However, a critical discrepancy has emerged between the primary optimization objectives of these codecs and their application in semantic generation tasks. When representations optimized solely for acoustic fidelity are applied for semantic tasks, they may exhibit semantic deficiencies [21] that compromise linguistic preservation, and may also be sensitive to perturbations [22], such as temporal slicing and phase pertur-

bation [20]. To address this, recent research has focused on integrating auxiliary losses into the **codec encoder** to enforce discrete representation consistency during training. One of the most prominent approaches is **semantic encoder distillation (SED)** [4, 21, 23]<sup>2</sup>, which aligns the codec’s quantized representations with those of a **self-supervised representation (SSR)** learning model [25–28]. Another method involves feeding an additional consistency loss to the codec encoder, enforcing consistency through perceptually invariant augmentations such as slicing or phase augmentation [20, 22]. These distillation and auxiliary-loss approaches demonstrate superior generative performance compared to acoustic-only-trained codecs [4, 21, 22]. However, these semantic encoder distillation methods do not guarantee the intelligibility or semantic consistency of the decoder’s output. A key reason is that these methods focus solely on the encoder and impose no loss on the decoder, thereby failing to ensure the intelligibility of the reconstructed audio. Several papers have already highlighted a semantic-acoustic conflict [4, 29], noting that codecs trained with semantic distillation often suffer from acoustic quality issues, particularly at low bitrates. Critically, low-bps models are typically evaluated against bitrate-constrained acoustic models without reporting intelligibility objective metrics such as WER.

Rather than using SED, SSR can be treated directly as a reconstruction target, similar to the mel-spectrogram, and it consists of differentiable modules. We refer to this objective as the **self-supervised representation reconstruction (SSRR)**. While conceptually similar to perceptual loss functions in the image domain [30] and speech enhancement [31], the only prior work that applies this strategy in neural audio codecs is TAAE [14]. However, TAAE applies SSRR only at the final stage of training and reports relatively low intelligibility. Moreover, it does not provide clear evidence on how SSRR contributes to improving training dynamics. In addition, due to relatively large model size and CPU-bounded operations, recent models, such as W2V-Bert 2.0 [28], are not commonly used.

The emergence of speech-to-speech models [4, 32] necessitates fully streaming codecs for real-time applications. While existing streaming models [4, 7, 12, 13, 16] have achieved competitive results, some rely on a large frame size [4], while others require lookahead mechanisms [13, 16] to maintain quality, thereby compromising low-latency requirements. Even with causal distillation techniques, streaming models often exhibit lower intelligibility than their non-streaming counterparts [16]. Architectures like TS3-Codec [12], which use Transformer-only designs, offer low computational cost but suffer from lim-

<sup>\*\*</sup>indicates the corresponding author.

<sup>1</sup><https://github.com/jhcodec843/jhcodec>

<sup>2</sup>We acknowledge the controversy surrounding the terminology ‘semantic’ [24], but we use it for consistency with previous literature.

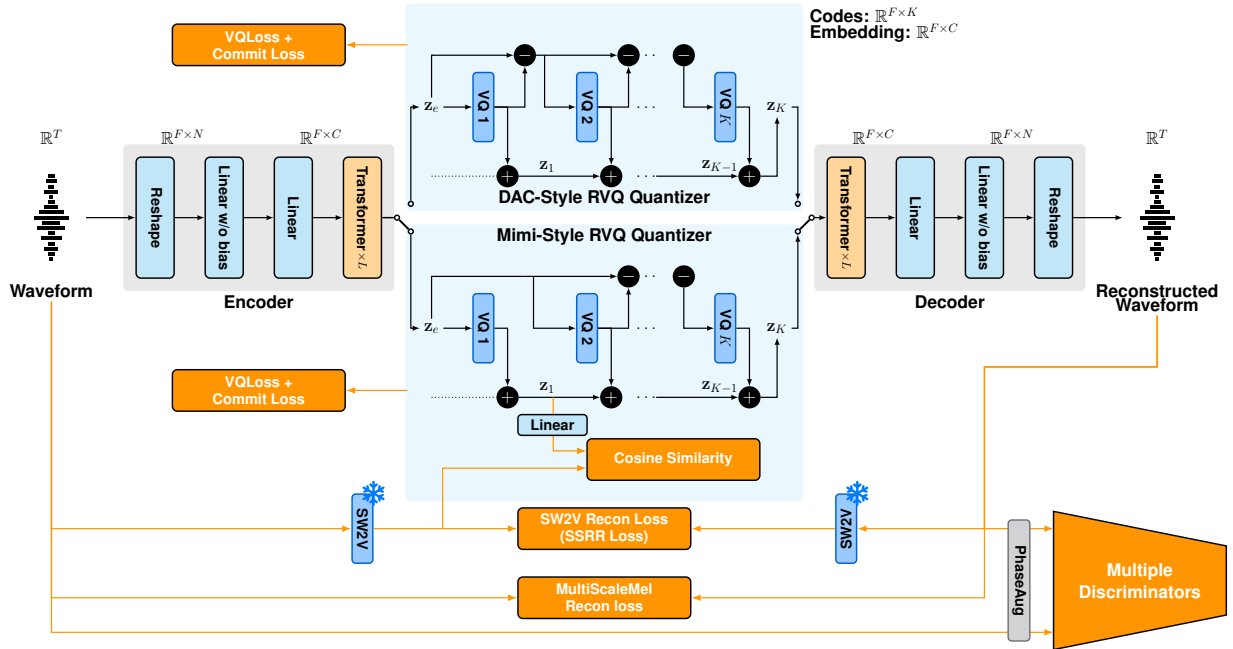


Figure 1: Overall system architecture of *JHCodec*, illustrating the two RVQ variants, DAC-style and Mimi-style.

ited bitrates and semantics-less training, leading to low intelligibility. MagiCodec [13] attempts to mitigate this with multi-stage training and masking, but it still faces similar challenges. It is also worth noting that some approaches apply streaming only to the decoder [33], but such codecs are not fully streamable, limiting their application to real-time speech-to-speech models.

In this work, we propose **JHCodec**, a streaming Transformer-based neural audio codec that prioritizes high-intelligibility reconstruction under strict low-latency constraints. Although recent codecs emphasize performance on downstream generative tasks, evidence from the image domain suggests that downstream quality is not always strongly correlated with reconstruction quality [34–36]. At the same time, prior studies indicate that pure reconstruction quality can serve as an upper bound for generation, with generation quality being further improved by training details [37]. Motivated by this perspective, we focus on reconstruction quality, particularly intelligibility, while ensuring low latency operation for practical speech applications. To this end, we adopt a high-bitrate, zero-lookahead architecture and introduce the SSRR loss to guide optimization toward linguistically meaningful representations rather than purely mel-spectrogram reconstruction. Unlike prior work that applies similar losses only in the later training stage and primarily evaluates signal-level metrics, we systematically study the effect of SSRR from early training across multiple RVQ configurations, with a focus on intelligibility (WER).

Our experiments show that SSRR substantially accelerates codec training, particularly during the early stages, while consistently improving all speech-related metrics. Notably, SSRR leads to significant gains in intelligibility under all bitrate settings by redefining the optimization objective toward linguistically meaningful representations rather than the mel-spectrogram. Moreover, incorporating SSRR enables efficient training with only one or two GPUs while achieving performance competitive with state-of-the-art baselines trained with large-scale, multi-node budgets. Overall, these results demon-

strate that SSRR is an effective and practical component for neural audio codecs, enabling our **JHCodec** to achieve state-of-the-art performance while maintaining extremely low latency.

## 2. Method

### 2.1. Model Architecture

We adopt the fully causal Transformer architecture, inspired by TS3-Codec [12], accelerated by FlashAttention [38, 39] optimization for low latency. Furthermore, despite the large parameter count of TS3-Codec, it demonstrates high computational efficiency with a low number of multiply-accumulate operations (MAC). Our architecture is built upon TS3-Codec by replacing its single-codebook VQ with RVQ and by reducing window sizes for improved computational efficiency. We also incorporate modern Transformer design principles, including Pre-Layer Normalization (PreLN) [40], rotary positional embeddings [41], SwiGLU activation for feed-forward networks [42], and LayerScale [43]. To enhance training stability, we retain LayerNorm [44] instead of replacing it with RMSNorm [45]. Figure 1 illustrates the overall architecture and the applied losses.

Specifically, our model utilizes an  $N = 320$ -sample window for input reshaping. This representation is then sequentially upsampled to 768 and subsequently to  $C = 1024$  dimensions using two linear layers. The encoder and decoder components each comprise  $L = 8$  Transformer decoder layers. Within these Transformer layers, we use a model dimension of 1024, which is expanded to 4096 in the feed-forward network (FFN). Additionally, all sliding window sizes are reduced to 16.

Reducing the frame rate in neural audio codecs improves computational efficiency but introduces a trade-off with intelligibility, as observed in TS3-Codec [12] and other prior studies [46]. To compensate for degraded intelligibility at low frame rates, such as 12.5 Hz, recent state-of-the-art codecs adopt deep RVQ hierarchies. For instance, Mimi [4] employs 32 codebooks. However, combining a low frame rate with deep RVQ

introduces two critical issues. First, a lower frame rate increases overall system latency, as each frame spans a longer temporal interval, thereby increasing the latency before decoding can proceed. Second, deep RVQ hierarchies significantly increase computational cost and latency due to repeated in-and-out projections across multiple quantization stages. These sequential quantization steps cannot be fully parallelized, further exacerbating the efficiency overhead. Moreover, for downstream speech-to-speech applications, Mimi is commonly configured with only 8 codebooks [4], since using all 32 results in substantial computational overhead. Therefore, we select a 50 Hz high frame rate configuration with  $K = 8$  codebooks to achieve high intelligibility while maintaining low latency.

To improve the system’s overall computational efficiency, we applied FlashAttention [38, 39] for all attentions. Notably, while some prior models do not provide an official streaming implementation, our model supports efficient streaming inference via KV caching [47].

## 2.2. Self-Supervised Representation

Previous studies have indicated that generating audio from semantic representations can enhance intelligibility [5, 23]. Following this, Mimi [4] explored distilling semantic information from WavLM [27] into the first VQ codebooks via cosine similarity. Without lookahead mechanisms, causal representations exhibit a high phoneme error rate, suggesting a distinct pattern compared to non-causal models [48]. Consequently, our objective is to extract a reliable, causal, and lightweight self-supervised speech representation.

To achieve this, we train an explicit model that distills self-supervised representations as causally as possible. Similar to Mimi’s SED approach [4], our causal model is trained to maximize the cosine similarity with the original self-supervised model’s representations. We choose multilingually trained W2V-BERT 2.0 (SW2V)<sup>3</sup> [28] for potential future multilingual extensions, as WavLM [27] is trained only on English datasets, which may limit multilingual generalization. Consistent with prior work [49], we utilize features from the 17th layer of W2V-BERT 2.0. In addition, since W2V-BERT 2.0 also uses 1024-dimensional embeddings, identical to our model’s dimensions, no additional layers are required to align its representation dimensionality with our model. The distilled causal self-supervised representation extractor shares the same architectural design as our codec’s encoder to achieve both efficient calculation and causal architecture. For brevity, we refer to this model as **SW2V**.

## 2.3. RVQ-VAE Neural Audio Codec

We adopt a neural audio compression framework based on the residual vector quantized variational auto-encoder (RVQ-VAE), drawing inspiration from prominent codecs such as DAC [8] and Mimi [4]. The model architecture consists of an encoder  $E$ , a quantizer  $Q$ , and a decoder  $G$ . Given a raw audio waveform  $\mathbf{x} \in \mathbb{R}^T$ , the encoder maps it to a sequence of continuous latent representations  $\mathbf{z}_e = E(\mathbf{x}) \in \mathbb{R}^{F \times C}$ , where  $T$  is the number of audio samples,  $F$  represents the number of frames, and  $C$  denotes the embedding channel dimension. Since quantization is applied independently to each frame in the  $F$ -length sequences, we simply describe the formulation at the frame level for clarity. For brevity, we omit the frame index and denote  $\mathbf{z}_e \in \mathbb{R}^C$  in the following derivations.

To quantize the continuous latent representations  $\mathbf{z}_e$  from the encoder, we employ RVQ. The quantizer  $Q$  comprises a sequence of  $K$  vector quantizers  $\{q_1, \dots, q_K\}$ . The quantization process is performed iteratively, where the input of the  $i$ -th quantizer is the residual error from the preceding stages, denoted as  $\mathbf{r}_i$ , and the corresponding quantized embedding is  $\tilde{\mathbf{z}}_i$ , defined as:

$$\mathbf{r}_1 = \mathbf{z}_e, \mathbf{r}_i = \mathbf{r}_{i-1} - \tilde{\mathbf{z}}_{i-1} = \mathbf{z}_e - \sum_{j=1}^{i-1} \tilde{\mathbf{z}}_j \quad \text{for } 2 \leq i \leq K. \quad (1)$$

To enhance robustness and enable variable bitrate operation, we adopt quantization dropout, proposed by Kumar *et al.* [8], in which only the first  $k$  quantizers are used, with  $1 \leq k \leq K$ . Under this quantization dropout scheme, the quantized representation using the first  $k$  quantizers is defined as:

$$\mathbf{z}_k = Q(\mathbf{z}_e) = \sum_{i=1}^k \tilde{\mathbf{z}}_i, \quad \text{where } \tilde{\mathbf{z}}_i = q_i(\mathbf{r}_i). \quad (2)$$

Furthermore, Kumar *et al.* [8] advocate for the use of input and output projections [50] during residual quantization to increase the codebook utilization, expressed as:

$$q_i(\mathbf{r}_i) = \mathbf{W}_{i,\text{out}} \mathbf{e}_{i,v_i}, \quad \text{where } v_i = \underset{j}{\operatorname{argmin}} \|\mathbf{W}_{i,\text{in}} \mathbf{r}_i - \mathbf{e}_{i,j}\|_2. \quad (3)$$

Here, the  $i$ -th vector quantizer consists of an input projection  $\mathbf{W}_{i,\text{in}} \in \mathbb{R}^{C \times M}$ , an output projection  $\mathbf{W}_{i,\text{out}} \in \mathbb{R}^{M \times C}$ , the  $i$ -th VQ quantizer with codebooks  $\{\mathbf{e}_{i,1}, \mathbf{e}_{i,2}, \dots, \mathbf{e}_{i,V}\}$ , the closest codebook index  $v_i \in \{1, 2, \dots, V\}$ . In this formulation,  $M$  is significantly smaller than  $C$  to achieve low-rank compression, and  $V$  denotes the codebook’s vocabulary size. We set  $M = 16$ , following the low-dimensional configuration of TS3-Codec [12]. In addition, we use the Euclidean distance VQ, rather than the cosine similarity VQ.

During the VQ, to enable gradient propagation between a vector quantizer, we employ the straight-through estimation (STE) [9]. When input and output projection layers are introduced [50], the gradient flow through  $q_i$  is given by:

$$\begin{aligned} \frac{\partial q_i(\mathbf{r}_i)}{\partial \mathbf{r}_i} &= \frac{\partial \tilde{\mathbf{z}}_i}{\partial \mathbf{r}_i} = \frac{\partial(\mathbf{W}_{i,\text{out}} \mathbf{e}_{i,v_i})}{\partial \mathbf{e}_{i,v_i}} \frac{\partial \mathbf{e}_{i,v_i}}{\partial(\mathbf{W}_{i,\text{in}} \mathbf{r}_i)} \frac{\partial(\mathbf{W}_{i,\text{in}} \mathbf{r}_i)}{\partial \mathbf{r}_i} \\ &= \mathbf{W}_{i,\text{out}}^\top \frac{\partial \mathbf{e}_{i,v_i}}{\partial(\mathbf{W}_{i,\text{in}} \mathbf{r}_i)} \mathbf{W}_{i,\text{in}}^\top \approx \mathbf{W}_{i,\text{out}}^\top \mathbf{W}_{i,\text{in}}^\top, \end{aligned} \quad (4)$$

where  $\frac{\partial \mathbf{e}_{i,v_i}}{\partial(\mathbf{W}_{i,\text{in}} \mathbf{r}_i)}$  is approximated to the identity matrix  $\mathbf{I}$  through the STE. Therefore, the gradient through the quantizer  $Q$  to the continuous latent, including quantizer drop can be represented as follows:

$$\begin{aligned} \frac{\partial \mathbf{z}_k}{\partial \mathbf{z}_e} &= \frac{\partial \left( \sum_{i=1}^k \tilde{\mathbf{z}}_i \right)}{\partial \mathbf{z}_e} = \sum_{i=1}^k \frac{\partial \tilde{\mathbf{z}}_i}{\partial \mathbf{r}_i} \frac{\partial \mathbf{r}_i}{\partial \mathbf{z}_e} \\ &\approx \left( \mathbf{W}_{1,\text{out}}^\top \mathbf{W}_{1,\text{in}}^\top \right. \\ &\quad \left. + \mathbf{W}_{2,\text{out}}^\top \mathbf{W}_{2,\text{in}}^\top (\mathbf{I} - \mathbf{W}_{1,\text{out}}^\top \mathbf{W}_{1,\text{in}}^\top) + \dots \right) \\ &= \left( \sum_{i=1}^k \mathbf{W}_{i,\text{out}}^\top \mathbf{W}_{i,\text{in}}^\top \left( \prod_{\substack{j=1, \\ \text{if } i > 1 \\ \text{else } \mathbf{I}}}^{i-1} (\mathbf{I} - \mathbf{W}_{j,\text{out}}^\top \mathbf{W}_{j,\text{in}}^\top) \right) \right). \end{aligned} \quad (5)$$

<sup>3</sup><https://hf.co/facebook/w2v-bert-2.0>

We backpropagate gradients through the encoder only via the quantized embeddings, unlike Mimi [4], which uses unquantized embeddings.

In addition, the RVQ module is trained using the standard VQ loss and commitment loss to jointly update the encoder and the codebooks. Specifically, we adopt the loss formulation from [9], which encourages the encoder outputs to commit to discrete codebook entries while allowing the codebooks to adapt to the data distribution. Both losses are as follows:

$$\mathcal{L}_{\text{vq}} = \sum_{i=1}^k \|\text{sg}[\mathbf{W}_{i,\text{in}}\mathbf{r}_i] - \mathbf{e}_{i,v_i}\|_2^2, \quad (6)$$

$$\mathcal{L}_{\text{commit}} = \sum_{i=1}^k \|\mathbf{W}_{i,\text{in}}\mathbf{r}_i - \text{sg}[\mathbf{e}_{i,v_i}]\|_2^2, \quad (7)$$

where sg refers to the stop gradient operation.

Mimi [4] integrates SED into DAC’s RVQ, employing two types of codebooks: acoustic and semantic. The acoustic codebooks operate identically to DAC’s RVQ. The semantic codebook utilizes only one VQ layer and applies a cosine similarity loss derived from a self-supervised model. The final quantized embedding is obtained by summing the outputs of these two components. While the original Mimi used WavLM [27], we use a distilled causal SW2V, as described in section 2.2. Furthermore, unlike direct WavLM distillation, which would require learning causal inference from a bi-directional model, SW2V inherently serves as an upper limit for a causal model’s performance. In particular, since the semantic representations from the Mimi-style semantic codec are quantized, they cannot match the performance of the continuously trained SW2V.

To compare DAC-style and Mimi-style RVQ setups within the TS3-Codec-based Transformer architecture, we trained both models with identical configurations, differing only in the RVQ setup. For both RVQ-style, we utilize vocabulary size of  $V = 1024$  for each codebook, and we employ  $K = 8$  codebooks.

The resulting quantized embedding  $\mathbf{z}_k$  is then fed into the decoder to synthesize the reconstructed waveform  $\hat{\mathbf{x}} = G(\mathbf{z}_k)$ . The model is trained with a comprehensive objective function that includes a multi-scale mel reconstruction loss with L1 distance  $\mathcal{L}_{\text{mel}}$  [3], adversarial losses  $\mathcal{L}_{\text{adv}}$ , and feature-matching losses  $\mathcal{L}_{\text{fm}}$  derived from discriminators. We utilize the multiple discriminators following MPD [19] and MS-STFTD [7]. In addition, phase perturbation has already shown effectiveness in both vocoder [20] and codec training [22]. We apply PhaseAug<sup>4</sup> as a differentiable GAN augmentation. The overall training objective follows the standard loss formulation for the neural audio codec is expressed as:

$$\begin{aligned} \mathcal{L}_{\text{codec}} = & \lambda_{\text{mel}}\mathcal{L}_{\text{mel}} + \lambda_{\text{vq}}\mathcal{L}_{\text{vq}} + \lambda_{\text{commit}}\mathcal{L}_{\text{commit}} \\ & + \lambda_{\text{adv}}\mathcal{L}_{\text{adv}} + \lambda_{\text{fm}}\mathcal{L}_{\text{fm}}, \end{aligned} \quad (8)$$

where  $\lambda_{\text{mel}}$ ,  $\lambda_{\text{vq}}$ ,  $\lambda_{\text{commit}}$ ,  $\lambda_{\text{adv}}$  and  $\lambda_{\text{fm}}$  are loss coefficients. The overall model is illustrated in Figure 1.

To make our codec more robust to noise, we add a small amount of noise to the encoder input, as GAN-based training has been shown to enable implicit upsampling [4] and denoising [6]. For 10% of the training batches, we randomly add either Gaussian or sinusoidal noise to encourage the model to implicitly learn to denoise stationary noise.

<sup>4</sup><https://github.com/maum-ai/phaseaug>

## 2.4. Self-Supervised Representation Reconstruction Loss

Despite the impressive reconstruction results of neural audio codecs, extensive research indicates that VQ often degrades intelligibility and speaker similarity compared to continuous features [51–53], particularly in streaming models. One reason is that, in the current loss  $\mathcal{L}_{\text{codec}}$ , intelligibility is influenced only indirectly through the multi-scale mel-spectrogram reconstruction loss and the feature-matching losses. Although a zero-valued loss would trivially correspond to identical intelligibility, the loss magnitude does not directly reflect the perceptual or linguistic intelligibility of the output speech.

To mitigate this limitation in the loss of the neural audio codec, we introduce the **self-supervised representation reconstruction (SSRR) loss** ( $\mathcal{L}_{\text{ssrr}}$ ), a more intuitive proxy for intelligibility based on the distance between self-supervised representations, explicitly capturing linguistic consistency beyond low-level acoustic similarity. We set the SW2V as the target representation. This loss quantifies and penalizes the semantic discrepancy between the original audio  $\mathbf{x}$  and the reconstructed audio  $\hat{\mathbf{x}}$ :

$$\mathcal{L}_{\text{ssrr}} = \|\Phi(\mathbf{x}) - \Phi(\hat{\mathbf{x}})\|_1. \quad (9)$$

Here,  $\Phi(\cdot)$  represents the operation of extracting features from the frozen SW2V. We adopt the L1 loss rather than the cosine similarity loss from SED, as the existing perceptual losses [14, 30, 31] and feature-matching losses [19] are known to be effective with the L1 or L2 loss, despite their target feature extractors being trained on different objectives.

By minimizing this objective, the gradient propagates backward through the decoder  $G$ , the quantizer  $Q$ , and the encoder  $E$ , compelling the codec to retain the phonetic information necessary to accurately reconstruct the SW2V features. While the standard GAN ( $\mathcal{L}_{\text{adv}}$  and  $\mathcal{L}_{\text{fm}}$ ) and multi-scale mel reconstruction losses ( $\mathcal{L}_{\text{mel}}$ ) do not explicitly guarantee the preservation of phonetic content under the quantizer drop,  $\mathcal{L}_{\text{ssrr}}$  explicitly enforces the retention of phonetic information, thereby improving intelligibility. The total training objective is as follows:

$$\mathcal{L}_{\text{total}} = \mathcal{L}_{\text{codec}} + \lambda_{\text{ssrr}}\mathcal{L}_{\text{ssrr}}. \quad (10)$$

## 3. Experiments

### 3.1. Training Details

For all experiments, we used the AdamW optimizer [54] with a learning rate of  $1 \times 10^{-4}$  and a weight decay of  $1 \times 10^{-2}$ . All audio samples were resampled to 16 kHz. During training, utterances from the same speaker were concatenated to form fixed-length inputs of 10.24 seconds. All training runs used one H200 GPU, except for JHCodec-M-8 after 600k steps, which used two H200 GPUs. All batch sizes were set to the maximum values that fully utilize the available GPU memory.

During SW2V training, we used a batch size of 300 and trained for 60k steps, stopping before instability occurred. The resulting SW2V model achieved an average cosine similarity of 0.9 or higher on the LibriTTS-R development set.

A batch size of 42 was used during codec training. We set  $\lambda_{\text{mel}} = 0.1$ ,  $\lambda_{\text{vq}} = 1$ ,  $\lambda_{\text{commit}} = 0.1$ ,  $\lambda_{\text{adv}} = 1$ ,  $\lambda_{\text{fm}} = 1$ . The SSRR weight was set to  $\lambda_{\text{ssrr}} = 1$  when SSRR was enabled, and  $\lambda_{\text{ssrr}} = 0$  otherwise. For each batch, we tracked the vocabulary usage of every codebook using an exponential moving average (EMA) with a decay rate of 0.99. If the EMA usage of a codebook entry fell below 0.90, we expired and reinitialized that entry with a randomly selected vector from the current batch. For the first 10k steps, the model was trained without

GAN objectives and without the SSRR loss. We empirically found that jointly training with these components hinders training stability in the initial stages. From 10k to 100k steps, GAN training and the SSRR loss were enabled, and we applied masking by replacing 10% of both encoder and decoder inputs with special mask tokens. After 100k steps, the masking was removed, and training continued with the full set of objectives. Beyond 600k steps, we used two H200 GPUs and trained the model to 1M steps, which corresponds to 1.4M steps under a single-GPU setting.

Unlike the typical GAN training, we updated the generator before the discriminator as G→D to improve training stability. Using the conventional D→G update scheme led to unstable training on noisy datasets. Following VITS [55], we reduced the memory footprint of the discriminators by randomly slicing 2.56-second audio segments as inputs to the discriminators. Notably, the discriminators consumed significantly more GPU memory than the codec during training. It could also be observed that the batch size used for training SW2V is substantially larger than that used for the codec, even though SW2V consumes only about half the GPU memory.

### 3.2. Datasets

Our models were trained on diverse corpora to enhance its generalization for English varieties and beyond. We utilized the train-clean subsets of LibriTTS-R [56], the train subset of MLS-en [57], VCTK [58], LibriHeavy-Large [59,60], the clean subset of HiFi-TTS [61], LJSpeech [62], the speech subset of RAVDESS [63], and the English subset of Emilia [64]. We employed dataset balancing to increase the sampling probability of clean speech data.

For evaluation, we used the LibriSpeech [65] test-clean subset for clean speech and the test-other subset for noisy speech. To further assess robustness under extreme noise conditions, we also evaluated on the TITW-Hard test set [66]. We also assessed its generalization to multilingual scenarios by testing on the MLS’s non-English test sets [57], including Dutch, French, German, Italian, Polish, Portuguese, and Spanish.

### 3.3. Metrics

Codec-Superb [67] supports a wide range of downstream tasks and signal reconstruction metrics, but does not directly assess whether the core speech content is preserved during reconstruction. We also measured STOI [68], and it does not reflect intelligibility for similar but failed reconstruction. Therefore, we focus on metrics that are more relevant to speech synthesis. We report word error rate (WER) and character error rate (CER) as automatic speech recognition (ASR)-based proxy metrics for intelligibility, measured by Whisper Large-v3<sup>5</sup> [69]. Speaker similarity (S-SIM) is measured as the cosine similarity between WavLM speaker embeddings<sup>6</sup> [27] extracted from the original and reconstructed speech signals. Perceptual speech quality is evaluated using the UTMOS v2 [70]. For the TITW-Hard test set, we compare differential WER (dWER), i.e., the difference between the original and reconstructed speech transcriptions, as this dataset only contains transcripts from an outdated version of Whisper rather than ground-truth transcriptions.

<sup>5</sup><https://hf.co/openai/whisper-large-v3>

<sup>6</sup><https://hf.co/microsoft/wavlm-base-plus-sv>

### 3.4. Ablations

We conduct ablation studies on the LibriTTS test-clean set to analyze (1) the impact of RVQ design choices and (2) the effect of SSRR loss, using models trained for 300k and 600k steps. The suffix D and M indicate DAC-style and Mimi-style RVQ configurations, respectively. The numeric suffix denotes the number of codebooks utilized in the inference. Results at the maximum bitrate are summarized in Table 1, while results across all bitrates are illustrated in Figure 2.

Model	Steps	SED	SSRR	WER (↓)	CER (↓)	S-SIM (↑)	UTMOS (↑)
Ground Truth (GT)	–	–	–	2.99	1.13	1.0000	3.2311
JHCodec-D-8	300k	✗	✗	6.28	3.15	0.9287	<b>3.3143</b>
JHCodec-D-8	300k	✗	✓	<b>3.54</b>	<b>1.38</b>	<b>0.9631</b>	3.2100
JHCodec-M-8	300k	✓	✗	5.43	2.48	0.9290	<b>3.2030</b>
JHCodec-M-8	300k	✓	✓	<b>3.57</b>	<b>1.50</b>	<b>0.9698</b>	3.1712
JHCodec-D-8	600k	✗	✓	3.31	1.31	0.9759	<b>3.2663</b>
JHCodec-M-8	600k	✓	✓	<b>3.29</b>	<b>1.29</b>	<b>0.9783</b>	3.1697
JHCodec-M-8	1M	✓	✓	<b>3.19</b>	<b>1.25</b>	<b>0.9826</b>	<b>3.3229</b>

Table 1: Evaluation results for JHCodec ablation study.

At 300k steps, before full convergence, the Mimi-style RVQ achieves lower WER and CER than the DAC-style RVQ without SSRR, indicating greater robustness to incomplete optimization. When SSRR is applied at 300k steps, both RVQ designs exhibit substantial gains in intelligibility and speaker similarity. This improvement can be attributed to SSRR explicitly regularizing discrete representations to be invariant to self-reconstruction, thereby mitigating quantization noise and preventing unstable codebook assignments during early training. As a result, SSRR reduces representation drift across frames and enforces more linguistically consistent tokenization, leading to more reliable downstream decoding. Figure 2’s top row shows the effect of SSRR across different bitrates and RVQ configurations. Across all configurations, SSRR consistently improves intelligibility and speaker similarity. At 300k steps, SSRR reduces WER by nearly half for both RVQ designs, highlighting its importance in stabilizing discrete representations under limited training budgets.

While SSRR may slightly reduce UTMOS in some settings, the overall trade-off is favorable, as the gains in intelligibility and speaker similarity outweigh minor perceptual qualities. Furthermore, when using SSRR, both models achieve WERs that do not exceed the ground-truth WER by more than 1% after only 300k training steps, which corresponds to a very early stage of training. Overall, these results demonstrate that SSRR plays a more dominant role in improving reconstruction performance than previous losses, particularly in low- and mid-resource training regimes.

At 600k steps, both RVQ variants achieve comparable WER and CER, while the Mimi-style RVQ consistently yields slightly higher S-SIM. These results indicate that while the Mimi-style RVQ provides a stronger inductive bias in early training, the choice of RVQ becomes less critical as training progresses. Figure 2’s bottom row presents the results for 600k steps. Each additional codebook increases the bitrate by 0.5 kbps. While UTMOS already achieves sufficiently high scores (above 3), the model with Mimi-style RVQ consistently yielded slightly better WER and S-SIM at all bitrates. Based on these observations, we adopt the Mimi-style RVQ configuration for the final model. We also report results after 1M training steps. The 600k-step model, trained with a single GPU, already achieves competitive performance.

The overall gradient norm of the system is on the order of

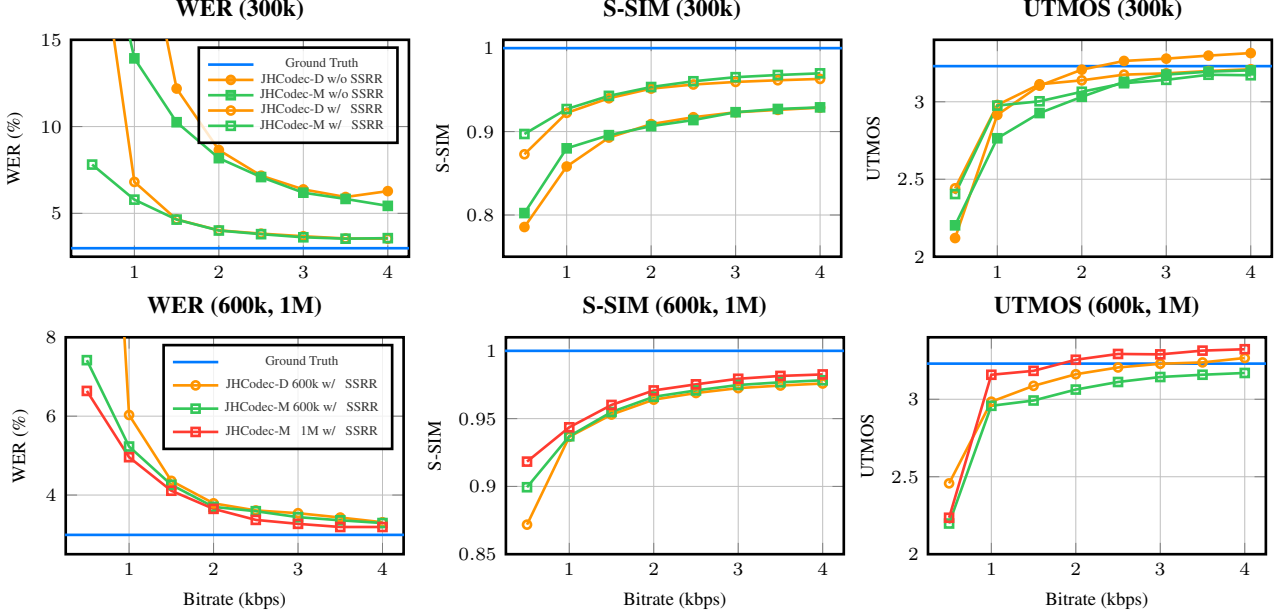


Figure 2: Ablation studies on audio codec performance. The top row analyzes the impact of self-supervised representation reconstruction (SSRR) loss at 300k iterations, while the bottom row compares residual vector quantization style (RVQ) at 600k and 1M iterations.

Model	# Parameters	Training GPU Budget	Streamable	Lookahead	SED	SSRR	Bitrate (kbps)	Frame Rate (Hz)	MAC (G)	Latency (ms)	RTF (Enc, Dec, Total)
Ground Truth (GT)	–	–	–	–	–	–	256.	–	–	–	–
<b>Non-Streaming</b>											
DAC-8	75M	N/A	✗	–	✗	✗	4.00	50	40.1	–	0.0008, 0.0011, 0.0019
BigCodec	159M	8 A100 × 600k steps	✗	–	✗	✗	1.04	80	67.1	–	0.0050, 0.0051, 0.0101
TAAE	950M	16 H100 × 650k+ steps	✗	–	✗	✓	0.70	25	37.4	–	0.0019, 0.0020, 0.0039
NanoCodec	62M	48 A100 × 196k steps	✗ <sup>†</sup>	–	✗	✗	1.78	12.5	48.5	–	0.0026, 0.0042, 0.0068
<b>Streaming</b>											
Mimi-32	79M	8 A100 × 1M steps	✓	0ms	✓	✗	4.40	12.5	8.1	86.7	0.0012, 0.0008, 0.0020
FocalCodec-Stream	249M	N/A	✓	60ms	✗	✗	0.80	50	13.5	80.0 <sup>‡</sup>	0.0012, 0.0005, 0.0017
MagiCodec	210M	N/A	✓	20ms	✗	✗	0.85	50	7.1	40.0 <sup>‡</sup>	<b>0.0005, 0.0004, 0.0009</b>
JHCodec-M-8	271M	<b>1 H200 × 1.4M steps</b>	✓	0ms	✓	✓	4.00	50	13.6	<b>26.8</b>	<b>0.0006, 0.0005, 0.0011</b>

Table 2: Comparisons with baseline codecs. <sup>†</sup> indicates that NanoCodec’s encoder is non-streamable while the decoder is streamable. <sup>‡</sup> refers to the minimum theoretical latency of the model. JHCodec-M achieves the lowest training GPU budget, full streamability, the lowest latency, and a competitive real-time factor.

$10^2$ , whereas standard Transformer decoders typically have gradient norms below 1. However, the model can still learn effective speech generation using the RVQ-VAE framework. We hypothesize that this behavior arises from the RVQ quantization formulation or suboptimal gradient flow from Eq. 5. Notably, we expect the norm of residual  $\mathbf{r}_k$  decreases as  $k$  increases. However, in practice, the residual norm does not consistently decrease. Moreover,  $\mathbf{I} - \mathbf{W}_{k,\text{out}}^T \mathbf{W}_{k,\text{in}}^T$  does not converge toward the zero matrix, as no explicit objective enforces this behavior. A more detailed analysis and potential remedies for this issue are left for future work.

### 3.5. Baselines

We compare our method with both non-streaming and streaming neural audio codecs. For non-streaming baselines, we evaluate DAC<sup>7</sup> [8], BigCodec<sup>8</sup> [11], TAAE<sup>9</sup> [14], and NanoCodec<sup>10</sup>

[33]. For streaming evaluation, we include Mimi<sup>11</sup> [4], MagiCodec<sup>12</sup> [13], and FocalCodec-Stream<sup>13</sup> [16]. While NanoCodec supports streaming at the decoder level, we categorize it as a non-streamable model since the overall system is not fully streamable. Unlike recent work that compares only low-bitrate setups, we compared a wide variety of codecs, including high-bitrate RVQ codecs. For RVQ-based codecs, the numeric suffix indicates the number of codebooks used. For Mimi, both the commonly used Mimi-8 and the maximum-capacity Mimi-32 configurations are reported. Table 2 shows the details of the baseline codecs.

Notably, prior codecs that report their training GPU budgets typically require more than 8 GPUs. Our codec is trained with 1 H200 GPU for the first 600k steps and with 2 H200 GPUs for the remaining 400k steps. For brevity, we report the total training budget as the equivalent of 1 H200 GPU for 1.4M steps.

To evaluate the computational efficiency of the proposed model, we measure the number of multiply-accumulate operations (MAC) based on a 1-second audio input. For temporal

<sup>7</sup>[https://hf.co/descript/dac\\_16khz](https://hf.co/descript/dac_16khz)

<sup>8</sup><https://hf.co/Alethia/BigCodec>

<sup>9</sup><https://hf.co/stabilityai/stable-codec-speech-16k>

<sup>10</sup><https://hf.co/nvidia/nemo-nano-codec-22khz-1.78kbps-12.5fps>

<sup>11</sup><https://hf.co/kyutai/mimi>

<sup>12</sup>[https://hf.co/Ereboas/MagiCodec\\_16k\\_50hz](https://hf.co/Ereboas/MagiCodec_16k_50hz)

<sup>13</sup>[https://hf.co/lucadellalib/focalcodec\\_50hz\\_65k\\_causal](https://hf.co/lucadellalib/focalcodec_50hz_65k_causal)

metrics, including latency and real-time factor (RTF), measurements are conducted over a 10-second duration to ensure stability. The reported latency is comprehensive, encompassing the time required for input frame buffering, the lookahead window, and the actual model processing time. Notably, the RVQ modules are found to significantly affect the total encoding time. This bottleneck arises because the iterative residual refinement in RVQ is inherently sequential, thereby preventing parallelization and dominating the inference cost.

Moreover, Transformer-decoder-only models, MagiCodec, and our JHCodec, exhibit very low real-time factors (RTF), indicating fast speech resynthesis. While FocalCodec-Stream and MagiCodec did not offer an optimized streaming codebase, we mark their theoretical minimum latency. While other models show high latency due to long frame lengths and lookahead, JHCodec achieves the lowest end-to-end latency due to its high frame rate and zero lookahead. As a result, JHCodec provides a practical advantage for real-time speech-to-speech systems, where minimizing codec latency is critical to overall latency.

### 3.6. Downstream Automatic Speech Recognition

To evaluate how well the discrete embedding preserves linguistic content, we trained automatic speech recognition (ASR) models using features extracted from the codec encoders and self-supervised models. This test also evaluates the quality of SW2V’s training. We fine-tune Whisper Small<sup>14</sup> [69] on top of codec features and report WER. Inputs are projected into the Whisper input space with an adapter composed of two convolutional layers followed by two transformer adapter layers. We train only the adapter for one epoch, then unfreeze the last two encoder and decoder layers of Whisper. Training uses LibriSpeech train-clean splits (460h) [65] with a batch size of 32, a learning rate of  $10^{-4}$  with 500 warmup steps, and 20 epochs. We tested models on the LibriSpeech test-clean dataset.

## 4. Results

### 4.1. LibriSpeech

Table 3 reports intelligibility, speaker similarity, and perceptual quality metrics on the LibriSpeech test-clean subset. Among non-streaming baselines, DAC-8 achieves strong intelligibility and speaker similarity, while BigCodec attains the highest perceptual quality in terms of UTMOS. For non-streaming baselines, NanoCodec and DAC-8 show competitive WER and CER, while BigCodec achieves the highest UTMOS score. Among the streaming baselines, Mimi-32 performs well on WER, CER, and S-SIM, ranking second-best in intelligibility metrics and best in speaker similarity, but yields lower UTMOS. Our proposed JHCodec-M-8 achieves a superior balance across all metrics. It ranks among the top-performing streaming models in WER, CER, and S-SIM while maintaining high perceptual quality. Notably, while NanoCodec utilizes a non-streaming encoder, JHCodec achieves the best WER and CER among fully streamable codecs, even outperforming Mimi-32 on clean data despite a significantly lower training budget.

While low-bitrate codecs generally exhibit slightly worse intelligibility metrics, BigCodec and MagiCodec achieve the highest perceptual quality among non-streaming and streaming, respectively. One possible explanation is that low-bitrate representations limit the capacity to preserve detailed linguistic information. As a result, models with limited complexity may

prioritize perceptual fidelity over intelligibility.

Model	WER (↓)	CER (↓)	S-SIM (↑)	UTMOS (↑)
Ground Truth (GT)	2.99	1.13	1.0000	3.2311
<b>Non-Streaming</b>				
DAC-8	<u>3.33</u>	<u>1.29</u>	0.9832	2.5845
BigCodec	3.67	1.50	0.9799	<b>3.3694</b>
TAAE	8.78	4.38	0.9371	<u>3.3495</u>
NanoCodec	<b>3.16</b>	<b>1.24</b>	<b>0.9886</b>	3.1630
<b>Streaming</b>				
Mimi-8	4.07	1.78	0.9673	2.7884
Mimi-32	<u>3.26</u>	<u>1.29</u>	<b>0.9898</b>	2.9685
FocalCodec-Stream	4.05	1.66	0.9606	2.9772
MagiCodec	4.35	1.85	0.9715	<b>3.4901</b>
<b>JHCodec-M-8</b>	<b>3.19</b>	<b>1.25</b>	<u>0.9826</u>	<u>3.3229</u>

Table 3: Evaluation results for JHCodec and baseline methods on the LibriSpeech test-clean dataset. For both streaming and non-streaming models, the best and second-best results are indicated in **bold** and underline, respectively.

Table 4 reports results on the test-other subset. Although intelligibility degrades across all codecs, it is especially severe in low-bitrate codecs. While performance degrades across all models, the trends remain consistent. Among non-streaming baselines, the tendency is similar, but DAC achieves the best speaker similarity. For streaming models, Mimi-32 achieves the best WER, CER, and speaker similarity, reflecting the benefit of higher RVQ capacity, while MagiCodec attains the highest UTMOS among streaming approaches. Our proposed JHCodec-M-8 demonstrates competitive, well-balanced performance across all metrics, ranking among the second-best streaming models for intelligibility, speaker similarity, and perceptual quality.

Model	WER (↓)	CER (↓)	S-SIM (↑)	UTMOS (↑)
Ground Truth (GT)	5.16	2.27	1.0000	2.9420
<b>Non-Streaming</b>				
DAC-8	<u>6.23</u>	<u>2.89</u>	<b>0.9812</b>	2.3838
BigCodec	8.22	4.10	0.9756	<b>3.0748</b>
TAAE	13.91	7.46	0.9312	<u>3.0550</u>
NanoCodec	<b>6.11</b>	<b>2.86</b>	<u>0.9682</u>	2.8308
<b>Streaming</b>				
Mimi-8	9.62	4.95	0.9626	2.4902
Mimi-32	<b>5.83</b>	<b>2.66</b>	<b>0.9874</b>	2.6489
FocalCodec-Stream	9.34	4.68	0.9536	2.7780
MagiCodec	10.65	5.61	0.9665	<b>3.2285</b>
<b>JHCodec-M-8</b>	<u>6.30</u>	<u>2.89</u>	<u>0.9780</u>	<u>2.9647</u>

Table 4: Evaluation results for the LibriSpeech test-other.

### 4.2. TITW-Hard Test

As shown in Table 5, all codecs exhibit substantial degradation for the TITW-Hard test set, particularly those at low bitrate codecs, where limited capacity struggles to resolve linguistic content from background noise. Among non-streaming baselines, DAC-8 achieves the lowest dWER and dCER, indicating strong robustness in terms of intelligibility, while BigCodec and TAAE prioritize perceptual quality, as reflected by higher UTMOS scores. For streaming models, Mimi-32 achieves the best intelligibility and speaker similarity, thanks to its higher RVQ capacity, whereas MagiCodec achieves the highest perceptual quality among streaming approaches. JHCodec-M-8 also demonstrates competitive and well-balanced performance across all metrics. Compared with the LibriSpeech test-clean

<sup>14</sup><https://huggingface.co/openai/whisper-small>

and test-other results, the same models remain the top two across all metrics, though their relative rankings change.

Model	dWER (↓)	dCER (↓)	S-SIM (↑)	UTMOS (↑)
Ground Truth (GT)	0.00	0.00	1.0000	2.5897
<b>Non-Streaming</b>				
DAC-8	<b>11.70</b>	<b>9.43</b>	<b>0.9628</b>	2.1863
BigCodec	18.77	14.58	0.9467	<b>2.7134</b>
TAAE	40.34	28.66	0.8224	<u>2.6022</u>
NanoCodec	<u>12.79</u>	<u>10.25</u>	<b>0.9683</b>	2.5647
<b>Streaming</b>				
Mimi-8	19.52	14.91	0.9296	2.3240
Mimi-32	<b>11.57</b>	<b>9.41</b>	<b>0.9740</b>	2.3998
FocalCodec-Stream	20.23	15.42	0.9165	2.5293
MagiCodec	20.10	15.37	0.9353	<b>2.9388</b>
<b>JHCodec-M-8</b>	<u>12.28</u>	<u>9.71</u>	<u>0.9549</u>	<u>2.6132</u>

Table 5: Evaluation results for TITW-Hard test dataset.

### 4.3. MLS-NonEnglish

We evaluate cross-lingual generalization on the MLS non-English test splits. Since JHCodec and several baselines are trained exclusively on English data, this benchmark assesses whether the learned representations generalize to linguistic structures beyond the training distribution. Among non-streaming codecs, NanoCodec and DAC-8 demonstrate relatively strong generalization, while TAAE shows a significant degradation, indicating limited robustness to cross-lingual variability. For streaming models, higher-capacity RVQ configurations such as Mimi-32 achieve the best intelligibility, suggesting that increased codebook capacity benefits multilingual reconstruction. Notably, JHCodec-M-8 achieves competitive WER and CER among all baselines, ranking consistently among the top performers. This result indicates that JHCodec’s discrete representations generalize reasonably well across languages, even though our model is trained exclusively on English speech. Overall, these findings suggest that the proposed codec maintains robust linguistic preservation across languages while satisfying streaming constraints.

Model	WER (↓)	CER (↓)
Ground Truth (GT)	6.73	2.31
<b>Non-Streaming</b>		
DAC-8	<u>7.64</u>	<u>2.69</u>
BigCodec	9.80	3.65
TAAE	52.72	28.79
NanoCodec	<b>7.50</b>	<b>2.62</b>
<b>Streaming</b>		
Mimi-8	11.35	4.45
Mimi-32	<b>7.30</b>	<b>2.55</b>
FocalCodec-Stream	11.48	4.59
MagiCodec	13.96	5.73
<b>JHCodec-M-8</b>	<u>7.44</u>	<u>2.65</u>

Table 6: Evaluation results for the MLS Non-English test splits.

### 4.4. Downstream Automatic Speech Recognition

Table 7 summarizes the downstream ASR results. Among the non-streaming self-supervised representations, WavLM outperforms W2V-BERT 2.0, likely because we evaluate the full WavLM model, whereas W2V-BERT 2.0 uses a partial configuration, and because WavLM is trained solely on English data. Similarly, our SW2V achieves the best WER among self-supervised representations, potentially reflecting training

bias, yet indicating linguistic modeling capability. Among the codec representations, DAC performs best despite not being trained with self-supervised objectives. Compared with Mimi and NanoCodec, JHCodec demonstrates superior performance.

Model	WER (↓)	CER (↓)
Whisper Small	3.44	1.24
<b>Non-Streaming</b>		
W2V2 (Full)	<u>4.73</u>	<b>2.17</b>
W2V-BERT 2.0 (17th)	4.94	2.92
WavLM-Large (Full)	<b>4.23</b>	<u>2.74</u>
DAC-8	<b>5.00</b>	<b>2.60</b>
NanoCodec	7.26	4.03
<b>Streaming</b>		
<b>SW2V</b>	<b>4.11</b>	<b>1.98</b>
Mimi-32	8.75	5.48
<b>JHCodec-M-8</b>	<b>5.53</b>	<b>3.04</b>

Table 7: Codec evaluation results for the downstream ASR.

### 4.5. Overall

Several key observations emerge across the evaluations. First, regarding efficiency and low latency, JHCodec-M-8 achieves state-of-the-art performance, even outperforming Mimi-32 on clean data, despite a significantly lower training budget. Second, our analysis of the trade-off between intelligibility and quality reveals that while models such as BigCodec, TAAE, and MagiCodec often prioritize perceptual quality at the expense of WER, JHCodec provides a more consistent balance across both categories. Third, due to the “semantic-acoustic conflict” observed in prior work, Mimi often achieves lower UTMOS, among all test sets compared to GT, but JHCodec, thanks to SSRR and denoising training, shows good UTMOS slightly higher than GT. Finally, DAC-8, NanoCodec, Mimi-32, and our JHCodec-M-8 achieve state-of-the-art performance, though their relative rankings vary across benchmarks.

## 5. Discussion

Our results suggest that incorporating **self-supervised representation reconstruction** (SSRR) significantly benefits final performance and the training dynamics of streaming neural audio codecs. Far from being a simple auxiliary objective, SSRR appears to play a key role in balancing intelligibility and perceptual quality within a strict zero-lookahead streaming framework. We show that SSRR not only yields state-of-the-art performance but also significantly accelerates convergence. Remarkably, competitive results are achieved within 300k steps using a single GPU, eliminating the need for large-scale multi-GPU training commonly required by recent studies. This substantially lowers the computational barrier for future research in neural speech codecs, and we further support this goal by open-sourcing our full implementation.

Thanks to its zero-lookahead and low-latency architecture, the proposed JHCodec-M is particularly well-suited for real-time speech-to-speech systems. Unlike alternative designs that rely on larger frame sizes or explicit lookahead, thereby increasing total system latency, we achieve competitive performance while strictly maintaining low end-to-end latency.

Furthermore, the proposed framework is not limited to speech codecs. The same principle can be extended to general audio codecs by leveraging universal audio representations trained on large-scale datasets [71], potentially improving semantic consistency across broader acoustic domains.

## 6. Generative AI Use Disclosure

We used generative AI to polish grammar and improve the clarity of the submitted manuscript. We used generative AI for code auto-completion. All generated text and code were reviewed by the authors before integration.

## 7. Acknowledgment

This work was supported by the Office of the Director of National Intelligence (ODNI), Intelligence Advanced Research Projects Activity (IARPA), via the ARTS Program under contract D2023-2308110001. The views and conclusions contained herein are those of the authors and should not be interpreted as necessarily representing the official policies, either expressed or implied, of ODNI, IARPA, or the U.S. Government. The U.S. Government is authorized to reproduce and distribute reprints for governmental purposes notwithstanding any copyright annotation therein.

## 8. References

- [1] S. Chen, C. Wang, Y. Wu, Z. Zhang, L. Zhou, S. Liu, Z. Chen, Y. Liu, H. Wang, J. Li *et al.*, “Neural codec language models are zero-shot text to speech synthesizers,” *IEEE Transactions on Audio, Speech and Language Processing*, 2025.
- [2] E. Kharitonov, D. Vincent, Z. Borsos, R. Marinier, S. Girgin, O. Pietquin, M. Sharifi, M. Tagliasacchi, and N. Zeghidour, “Speak, read and prompt: High-fidelity text-to-speech with minimal supervision,” *Transactions of the Association for Computational Linguistics*, vol. 11, pp. 1703–1718, 2023.
- [3] J. Copet, F. Kreuk, I. Gat, T. Remez, D. Kant, G. Synnaeve, Y. Adi, and A. Défossez, “Simple and controllable music generation,” *NeurIPS*, vol. 36, pp. 47 704–47 720, 2023.
- [4] A. Défossez, L. Mazaré, M. Orsini, A. Royer, P. Pérez, H. Jégou, E. Grave, and N. Zeghidour, “Moshi: a speech-text foundation model for real-time dialogue,” *arXiv preprint arXiv:2410.00037*, 2024.
- [5] Z. Borsos, R. Marinier, D. Vincent, E. Kharitonov, O. Pietquin, M. Sharifi, D. Roblek, O. Teboul, D. Grangier, M. Tagliasacchi *et al.*, “Audiolm: a language modeling approach to audio generation,” *IEEE/ACM transactions on audio, speech, and language processing*, vol. 31, pp. 2523–2533, 2023.
- [6] N. Zeghidour, A. Luebs, A. Omran, J. Skoglund, and M. Tagliasacchi, “Soundstream: An end-to-end neural audio codec,” *IEEE/ACM Transactions on Audio, Speech, and Language Processing*, vol. 30, pp. 495–507, 2021.
- [7] A. Défossez, J. Copet, G. Synnaeve, and Y. Adi, “High fidelity neural audio compression,” *arXiv preprint arXiv:2210.13438*, 2022.
- [8] R. Kumar, P. Seetharaman, A. Luebs, I. Kumar, and K. Kumar, “High-fidelity audio compression with improved rvqgan,” *NeurIPS*, vol. 36, pp. 27 980–27 993, 2023.
- [9] A. Van Den Oord, O. Vinyals *et al.*, “Neural discrete representation learning,” *NeurIPS*, vol. 30, 2017.
- [10] S. Ji, Z. Jiang, W. Wang, Y. Chen, M. Fang, J. Zuo, Q. Yang, X. Cheng, Z. Wang, R. Li *et al.*, “Wavtokenizer: an efficient acoustic discrete codec tokenizer for audio language modeling,” *arXiv preprint arXiv:2408.16532*, 2024.
- [11] D. Xin, X. Tan, S. Takamichi, and H. Saruwatari, “Bigcodec: Pushing the limits of low-bitrate neural speech codec,” *arXiv preprint arXiv:2409.05377*, 2024.
- [12] H. Wu, N. Kanda, S. E. Eskimez, and J. Li, “Ts3-codec: Transformer-based simple streaming single codec,” *arXiv preprint arXiv:2411.18803*, 2024.
- [13] Y. Song, J. Chen, X. Zhuang, C. Du, Z. Ma, J. Wu, J. Cong, D. Jia, Z. Chen, Y. Wang *et al.*, “Magiccodec: Simple masked gaussian-injected codec for high-fidelity reconstruction and generation,” *arXiv preprint arXiv:2506.00385*, 2025.
- [14] J. D. Parker, A. Smirnov, J. Pons, C. Carr, Z. Zukowski, Z. Evans, and X. Liu, “Scaling transformers for low-bitrate high-quality speech coding,” *arXiv preprint arXiv:2411.19842*, 2024.
- [15] L. Della Libera, F. Paissan, C. Subakan, and M. Ravanelli, “FocalCodec: Low-bitrate speech coding via focal modulation networks,” in *NeurIPS*, 2025.
- [16] L. Della Libera, C. Subakan, and M. Ravanelli, “Focalcodecstream: Streaming low-bitrate speech coding via causal distillation,” *arXiv preprint arXiv:2509.16195*, 2025.
- [17] I. J. Goodfellow, J. Pouget-Abadie, M. Mirza, B. Xu, D. Warde-Farley, S. Ozair, A. C. Courville, and Y. Bengio, “Generative adversarial nets,” in *NeurIPS*, 2014.
- [18] K. Kumar, R. Kumar, T. De Boissiere, L. Gestin, W. Z. Teoh, J. Sotelo, A. De Brebisson, Y. Bengio, and A. C. Courville, “Melgan: Generative adversarial networks for conditional waveform synthesis,” *NeurIPS*, vol. 32, 2019.
- [19] J. Kong, J. Kim, and J. Bae, “Hifi-gan: Generative adversarial networks for efficient and high fidelity speech synthesis,” *NeurIPS*, vol. 33, pp. 17 022–17 033, 2020.
- [20] J. Lee, S. Han, H. Cho, and W. Jung, “PhaseAug: a differentiable augmentation for speech synthesis to simulate one-to-many mapping,” in *IEEE ICASSP*. IEEE, 2023, pp. 1–5.
- [21] Z. Ye, P. Sun, J. Lei, H. Lin, X. Tan, Z. Dai, Q. Kong, J. Chen, J. Pan, Q. Liu *et al.*, “Codec does matter: Exploring the semantic shortcoming of codec for audio language model,” in *Proceedings of the AAAI Conference on Artificial Intelligence*, vol. 39, no. 24, 2025, pp. 25 697–25 705.
- [22] W. Liu, Z. Guo, J. Xu, Y. Lv, Y. Chu, Z. Liu, and J. Lin, “Analyzing and mitigating inconsistency in discrete speech tokens for neural codec language models,” in *Proceedings of the 63rd Annual Meeting of the Association for Computational Linguistics (Volume 1: Long Papers)*, 2025, pp. 31 035–31 046.
- [23] X. Zhang, D. Zhang, S. Li, Y. Zhou, and X. Qiu, “Spechtokener: Unified speech tokenizer for speech large language models,” *arXiv preprint arXiv:2308.16692*, 2023.
- [24] K. Choi, A. Pasad, T. Nakamura, S. Fukayama, K. Livescu, and S. Watanabe, “Self-supervised speech representations are more phonetic than semantic,” in *Interspeech*, 2024.
- [25] A. Baevski, Y. Zhou, A. Mohamed, and M. Auli, “wav2vec 2.0: A framework for self-supervised learning of speech representations,” *NeurIPS*, vol. 33, pp. 12 449–12 460, 2020.
- [26] W.-N. Hsu, B. Bolte, Y.-H. H. Tsai, K. Lakhotia, R. Salakhutdinov, and A. Mohamed, “Hubert: Self-supervised speech representation learning by masked prediction of hidden units,” *IEEE/ACM transactions on audio, speech, and language processing*, vol. 29, pp. 3451–3460, 2021.
- [27] S. Chen, C. Wang, Z. Chen, Y. Wu, S. Liu, Z. Chen, J. Li, N. Kanda, T. Yoshioka, X. Xiao *et al.*, “Wavlm: Large-scale self-supervised pre-training for full stack speech processing,” *IEEE Journal of Selected Topics in Signal Processing*, vol. 16, no. 6, pp. 1505–1518, 2022.
- [28] L. Barrault, Y.-A. Chung, M. C. Meglioli, D. Dale, N. Dong, P.-A. Duquenne, H. Elsahar, H. Gong, K. Heffernan, J. Hoffman *et al.*, “Seamlessm4t: massively multilingual & multimodal machine translation,” *arXiv preprint arXiv:2308.11596*, 2023.
- [29] Y. Gong, L. Jin, R. Deng, D. Zhang, X. Zhang, Q. Cheng, Z. Fei, S. Li, and X. Qiu, “Xy-tokenizer: Mitigating the semantic-acoustic conflict in low-bitrate speech codecs,” *arXiv preprint arXiv:2506.23325*, 2025.
- [30] J. Johnson, A. Alahi, and L. Fei-Fei, “Perceptual losses for real-time style transfer and super-resolution,” in *European conference on computer vision*. Springer, 2016, pp. 694–711.

- [31] S. Kataria, J. Villalba, and N. Dehak, "Perceptual loss based speech denoising with an ensemble of audio pattern recognition and self-supervised models," in *IEEE ICASSP*. IEEE, 2021, pp. 7118–7122.
- [32] T. Labiausse, L. Mazaré, E. Grave, P. Pérez, A. Défossez, and N. Zeghidour, "High-fidelity simultaneous speech-to-speech translation," *arXiv preprint arXiv:2502.03382*, 2025.
- [33] E. Casanova, P. Neekhara, R. Langman, S. Hussain, S. Ghosh, X. Yang, A. Jukic, J. Li, and B. Ginsburg, "NanoCodec: Towards High-Quality Ultra Fast Speech LLM Inference," in *Interspeech*, 2025, pp. 5028–5032.
- [34] V. Ramanujan, K. Tirumala, A. Aghajanyan, L. Zettlemoyer, and A. Farhadi, "When worse is better: Navigating the compression-generation tradeoff in visual tokenization," *arXiv preprint arXiv:2412.16326*, 2024.
- [35] J. Yao, B. Yang, and X. Wang, "Reconstruction vs. generation: Taming optimization dilemma in latent diffusion models," in *Proceedings of the Computer Vision and Pattern Recognition Conference*, 2025, pp. 15 703–15 712.
- [36] L. Yu, J. Lezama, N. B. Gundavarapu, L. Versari, K. Sohn, D. Minnen, Y. Cheng, V. Birodkar, A. Gupta, X. Gu *et al.*, "Language model beats diffusion tokenizer is key to visual generation," *arXiv preprint arXiv:2310.05737*, 2023.
- [37] Y. Zhu, J. Chen, Y. Chen, Z. Chen, D. Jia, J. Cong, X. Zhuang, Y. Wang, and Y. Wang, "Heptapod: Language modeling on visual signals," *arXiv preprint arXiv:2510.06673*, 2025.
- [38] T. Dao, D. Fu, S. Ermon, A. Rudra, and C. Ré, "Flashattention: Fast and memory-efficient exact attention with io-awareness," in *NeurIPS*, vol. 35, 2022, pp. 16 344–16 359.
- [39] T. Dao, "Flashattention-2: Faster attention with better parallelism and work partitioning," in *ICLR*, 2024. [Online]. Available: <https://openreview.net/forum?id=mZn2Xyh9Ec>
- [40] R. Xiong, Y. Yang, D. He, K. Zheng, S. Zheng, C. Xing, H. Zhang, Y. Lan, L. Wang, and T. Liu, "On layer normalization in the transformer architecture," in *ICLR*, 2020.
- [41] J. Su, M. Ahmed, Y. Lu, S. Pan, W. Bo, and Y. Liu, "Roformer: Enhanced transformer with rotary position embedding," *Neuro-computing*, vol. 568, 2024.
- [42] N. Shazeer, "Glu variants improve transformer," *arXiv preprint arXiv:2002.05202*, 2020.
- [43] H. Touvron, M. Cord, A. Sablayrolles, G. Synnaeve, and H. Jégou, "Going deeper with image transformers," in *CVPR*, 2021.
- [44] J. L. Ba, J. R. Kiros, and G. E. Hinton, "Layer normalization," *arXiv:1607.06450*, 2016.
- [45] B. Zhang and R. Sennrich, "Root mean square layer normalization," *NeurIPS*, vol. 32, 2019.
- [46] J. Li, Y. Qian, Y. Hu, leying zhang, X. Wang, H. Lu, M. Thakker, J. Li, sheng zhao, and Z. Wu, "Flexicodec: A dynamic neural audio codec for low frame rates," in *ICLR*, 2026. [Online]. Available: <https://openreview.net/forum?id=kYkfCs4ZAH>
- [47] R. Pope, S. Douglas, A. Chowdhery, J. Devlin, J. Bradbury, J. Heek, K. Xiao, S. Agrawal, and J. Dean, "Efficiently scaling transformer inference," *Proceedings of machine learning and systems*, vol. 5, pp. 606–624, 2023.
- [48] Y. Meng, S. Goldwater, and H. Tang, "Effective context in neural speech models," *arXiv preprint arXiv:2505.22487*, 2025.
- [49] Z. Ye, X. Zhu, C.-M. Chan, X. Wang, X. Tan, J. Lei, Y. Peng, H. Liu, Y. Jin, Z. Dai *et al.*, "Llaza: Scaling train-time and inference-time compute for llama-based speech synthesis," *arXiv preprint arXiv:2502.04128*, 2025.
- [50] J. Yu, X. Li, J. Y. Koh, H. Zhang, R. Pang, J. Qin, A. Ku, Y. Xu, J. Baldridge, and Y. Wu, "Vector-quantized image modeling with improved vqgan," *arXiv preprint arXiv:2110.04627*, 2021.
- [51] J. Lee, W. Jung, H. Cho, J. Kim, and J. Kim, "PITS: Variational pitch inference without fundamental frequency for end-to-end pitch-controllable TTS," *arXiv preprint arXiv:2302.12391*, 2023.
- [52] X. Zhang, X. Zhang, K. Peng, Z. Tang, V. Manohar, Y. Liu, J. Hwang, D. Li, Y. Wang, J. Chan *et al.*, "Vevo: Controllable zero-shot voice imitation with self-supervised disentanglement," *arXiv preprint arXiv:2502.07243*, 2025.
- [53] J. Lee, H. Wang, Y. Guan, T. Thebaud, L. Moro-Velazquez, J. Villalba, and N. Dehak, "Maskvct: Masked voice codec transformer for zero-shot voice conversion with increased controllability via multiple guidances," *arXiv preprint arXiv:2509.17143*, 2025.
- [54] I. Loshchilov and F. Hutter, "Decoupled weight decay regularization," in *ICLR*, 2019.
- [55] J. Kim, J. Kong, and J. Son, "Conditional variational autoencoder with adversarial learning for end-to-end text-to-speech," in *ICML*. PMLR, 2021, pp. 5530–5540.
- [56] Y. Koizumi, H. Zen, S. Karita, Y. Ding, K. Yatabe, N. Morioka, M. Bacchiani, Y. Zhang, W. Han, and A. Bapna, "Libritts-r: A restored multi-speaker text-to-speech corpus," in *Interspeech*, 2023.
- [57] V. Pratap, Q. Xu, A. Sriram, G. Synnaeve, and R. Collobert, "Mls: A large-scale multilingual dataset for speech research," in *Interspeech*, 2020.
- [58] C. Veaux, J. Yamagishi, K. MacDonald *et al.*, "Superseded-ctr vctk corpus: English multi-speaker corpus for cstr voice cloning toolkit (Version 0.92)," 2016. [Online]. Available: <https://datashare.ed.ac.uk/handle/10283/3443>
- [59] J. Kahn, M. Rivière, W. Zheng, E. Kharitonov, Q. Xu, P. E. Mazaré, J. Karadayi, V. Liptchinsky, R. Collobert, C. Fuegen, T. Likhomanenko, G. Synnaeve, A. Joulin, A. Mohamed, and E. Dupoux, "Libri-light: A benchmark for asr with limited or no supervision," in *IEEE ICASSP*, 2020.
- [60] W. Kang, X. Yang, Z. Yao, F. Kuang, Y. Yang, L. Guo, L. Lin, and D. Povey, "Libriheavy: a 50,000 hours asr corpus with punctuation casing and context," *arXiv:2309.08105*, 2023.
- [61] E. Bakhturina, V. Lavrukhin, B. Ginsburg, and Y. Zhang, "Hi-Fi Multi-Speaker English TTS Dataset," in *Interspeech*, 2021.
- [62] K. Ito and L. Johnson, "The lj speech dataset," <https://keithito.com/LJ-Speech-Dataset>, 2017.
- [63] S. R. Livingstone and F. A. Russo, "The ryerson audio-visual database of emotional speech and song (ravdess): A dynamic, multimodal set of facial and vocal expressions in north american english," *PLoS one*, vol. 13, no. 5, 2018.
- [64] H. He, Z. Shang, C. Wang, X. Li, Y. Gu, H. Hua, L. Liu, C. Yang, J. Li, P. Shi *et al.*, "Emilia: An extensive, multilingual, and diverse speech dataset for large-scale speech generation," in *2024 IEEE SLT*. IEEE, 2024, pp. 885–890.
- [65] V. Panayotov, G. Chen, D. Povey, and S. Khudanpur, "Librispeech: an asr corpus based on public domain audio books," in *IEEE ICASSP*. IEEE, 2015, pp. 5206–5210.
- [66] J.-w. Jung, W. Zhang, S. Maiti, Y. Wu, X. Wang, J.-H. Kim, Y. Matsunaga, S. Um, J. Tian, H.-j. Shim *et al.*, "The text-to-speech in the wild (titw) database," *arXiv preprint arXiv:2409.08711*, 2024.
- [67] H. Wu, H.-L. Chung, Y.-C. Lin, Y.-K. Wu, X. Chen, Y.-C. Pai, H.-H. Wang, K.-W. Chang, A. Liu, and H.-y. Lee, "Codec-superb: An in-depth analysis of sound codec models," in *Findings of the Association for Computational Linguistics: ACL 2024*, 2024, pp. 10 330–10 348.
- [68] C. H. Taal, R. C. Hendriks, R. Heusdens, and J. Jensen, "A short-time objective intelligibility measure for time-frequency weighted noisy speech," in *IEEE ICASSP*, 2010, pp. 4214–4217.
- [69] A. Radford, J. W. Kim, T. Xu, G. Brockman, C. McLeavey, and I. Sutskever, "Robust speech recognition via large-scale weak supervision," in *ICML*. PMLR, 2023, pp. 28 492–28 518.
- [70] K. Baba, W. Nakata, Y. Saito, and H. Saruwatari, "The t05 system for the VoiceMOS Challenge 2024: Transfer learning from deep image classifier to naturalness MOS prediction of high-quality synthetic speech," in *IEEE SLT*, 2024.
- [71] B. Shi, A. Tjandra, J. Hoffman, H. Wang, Y.-C. Wu, L. Gao, J. Richter, M. Le, A. Vyas, S. Chen *et al.*, "Sam audio: Segment anything in audio," *arXiv preprint arXiv:2512.18099*, 2025.